

Wind accretion: Theory and Observations

N.I. Shakura¹, K.A. Postnov¹,
A.Yu. Kochetkova¹, L. Hjalmarsson¹,
L. Sidoli², A. Paizis²

¹ *Moscow M.V. Lomonosov State University,
Sternberg Astronomical Institute, 13, Universitetskij pr., 119992 Moscow, Russia*

² *INAF, Istituto di Astrofisica Spaziale e Fisica Cosmica,
Via E. Bassini 15, I-20133 Milano, Italy*

July 15, 2014

Abstract

A review of wind accretion in high-mass X-ray binaries is presented. We focus on different regimes of quasi-spherical accretion onto a neutron star: supersonic (Bondi) accretion, which takes place when the captured matter cools down rapidly and falls supersonically towards the neutron-star magnetosphere, and subsonic (settling) accretion which occurs when the plasma remains hot until it meets the magnetospheric boundary. The two regimes of accretion are separated by a limit in X-ray luminosity at about 4×10^{36} erg s⁻¹. In subsonic accretion, which works at lower luminosities, a hot quasi-spherical shell must form around the magnetosphere, and the actual accretion rate onto the neutron star is determined by the ability of the plasma to enter the magnetosphere due to the Rayleigh-Taylor instability. In turn, two regimes of subsonic accretion are possible, depending on the plasma cooling mechanism (Compton or radiative) near the magnetosphere. The transition from the high-luminosity regime with Compton cooling to the low-luminosity ($L_x \lesssim 3 \times 10^{35}$ erg s⁻¹) regime with radiative cooling can be responsible for the onset of the 'off' states repeatedly observed in several low-luminosity slowly accreting pulsars, such as Vela X-1, GX 301-2 and 4U 1907+09. The triggering of the transition may be due to a switch in the X-ray beam pattern in response to a change in the optical depth in the accretion column with changing luminosity. We also show that in the settling accretion theory, bright X-ray flares ($\sim 10^{38} - 10^{40}$ ergs) observed in supergiant fast X-ray transients (SFXT) may be produced by sporadic capture of magnetized stellar-wind plasma. At sufficiently low accretion rates, magnetic reconnection can enhance the magnetospheric plasma entry rate, resulting in copious production of X-ray photons, strong Compton cooling and ultimately in unstable accretion of the entire shell. A bright flare develops on the free-fall time scale in the shell, and the typical energy released in an SFXT bright flare corresponds to the mass of the shell.

1 Introduction

In 1966, one of us, Nikolay Ivanovich Shakura, was a 4th-year student at the Physical Department of Moscow State University, and heard for the first time the term ‘accretion’ from Yakov Borisovich Zeldovich. Yakov Borisovich suggested to Nikolay Ivanovich to study spherical accretion onto a neutron star (NS). Note that at that time neither radio pulsars, nor X-ray pulsars or accreting black holes were known – all these rich observational **appearances** of neutron stars and black holes were discovered later. When formulating this problem, Zeldovich was motivated by the discovery of galactic X-ray sources from rocket flights, such as Sco X-1. [1] (see the Nobel lecture by R. Giacconi [2] for an historical review).

During spherical accretion of gas onto a NS without magnetic field, a strong shock arises above the NS surface, the gas is heated up to a temperature of up to a few keV. The structure of this region and the emergent radiation spectrum was first calculated in [3]. While the mechanism of X-ray emission from a spherically accreting NS as proposed in that paper reproduced the main features of the observed X-ray spectra, the nature of galactic X-ray sources remained unclear until the launch of the first specialized UHURU satellite. UHURU discovered two main types of X-ray sources – those which show regular pulsations like Cen X-3 and Her X-1 (X-ray pulsars), and those with chaotic X-ray variability like Cyg X-1 (which turned out to be a black-hole candidate). Both are cases of accretion in a close binary system in which matter is transferred from the optical (non-degenerate) star overflowing its Roche lobe onto the compact object (a degenerate star or a black hole) with the formation of an accretion disk [4, 5].

¹.

2 Supersonic and subsonic wind accretion

Generally, in close binary systems, there can be two different regimes of accretion onto the compact object – disk accretion [9, 10, 11]² and quasi-spherical accretion. The disk accretion regime is usually realized when the optical star overfills its Roche lobe. Quasi-spherical accretion is most likely to occur in high-mass X-ray binaries (HMXB) when an optical star of early spectral class (O-B) does not fill its Roche lobe, but experiences a significant mass loss via its stellar wind. We shall discuss the wind accretion regime, in which a bow shock forms in the stellar wind around the compact star. The structure of the bow shock and the associated accretion wake is non-stationary and quite complicated (see e.g. numerical simulations [13, 14, 15], among many others). The characteristic distance at which the bow shock forms is approximately that of the Bondi radius $R_B = 2GM/(v_w^2 + v_{orb}^2)$, where v_w is the wind velocity (typically 100-1000 km/s) and v_{orb} is the orbital velocity of the compact star. In HMXBs, the stellar wind velocity is usually much larger than v_{orb} , so below we will neglect v_{orb} . The rate of gravitational capture of mass from a wind with density ρ_w near

¹Note that between the first discoveries of Galactic X-ray sources in 1962 and the UHURU observations, radio pulsars with non-trivial (and unclear up to now!) non-thermal mechanisms of radio emission were reported [6]. Soon they were recognized to be isolated rotating magnetized NS [7, 8]

²Accretion disks in active galactic nuclei were first considered by Lynden-Bell [12].

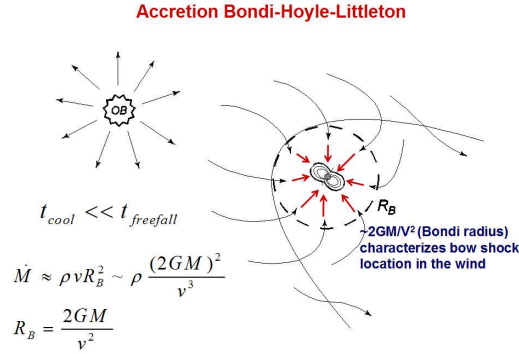


Figure 1: Supersonic (Bondi-Hoyle-Littleton) accretion onto magnetized NS

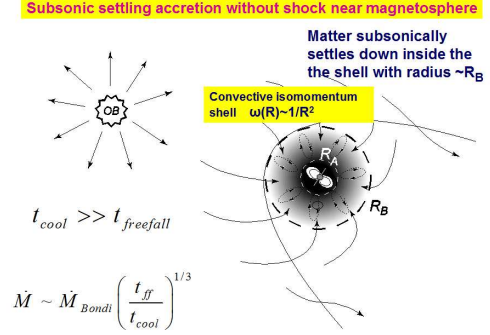


Figure 2: Subsonic settling accretion onto magnetized NS

the orbital position of the NS is the Bondi mass accretion rate: $\dot{M}_B \approx \rho_w R_B^2 v_w \propto \rho_w v_w^{-3}$.

Then, there are two different cases of quasi-spherical accretion. Classical Bondi-Hoyle-Littleton accretion takes place when the shocked matter is cooled down rapidly, and the matter falls freely towards the NS magnetosphere (see Fig. 1) by forming a shock at some distance above the magnetosphere. Here the shocked matter cools down (mainly via Compton processes) and enters the magnetosphere due to the Rayleigh-Taylor instability [16]. The magnetospheric boundary is characterized by the Alfvén radius R_A , which can be calculated from the balance between the ram pressure of the infalling matter and the magnetic field pressure at the magnetospheric boundary. The captured matter from the wind carries a specific angular momentum $j_w \sim \omega_B R_B^2$ [17]. Depending on the sign of j_w (prograde or retrograde), the NS can spin-up or spin-down. This regime of quasi-spherical accretion occurs in bright X-ray pulsars with $L_x > 4 \times 10^{36} \text{ erg s}^{-1}$ [18, 19].

If the captured wind matter behind the bow shock at R_B remains hot (which it does when the plasma cooling time is much longer than the free-fall time, $t_{cool} \gg t_{ff}$), a hot quasi-static shell forms around the magnetosphere and subsonic (settling) accretion sets in (see Fig. 2). In this case, both spin-up and spin-down of the NS is possible, even if the sign of j_w is positive (prograde). The shell mediates the angular momentum transfer from the NS magnetosphere via viscous stresses due to convection and turbulence. In this regime, the mean radial velocity of matter in the shell u_r is smaller than the free-fall velocity u_{ff} : $u_r = f(u)u_{ff}$, $f(u) < 1$, and is determined by the plasma cooling rate near the magnetosphere (due to Compton or radiative cooling): $f(u) \sim [t_{ff}(R_A)/t_{cool}(R_A)]^{1/3}$. In the settling accretion regime the actual mass accretion rate onto the NS may be significantly smaller than the Bondi mass accretion rate, $\dot{M} = f(u)\dot{M}_B$. Settling accretion occurs at $L_x < 4 \times 10^{36} \text{ erg s}^{-1}$ [19].

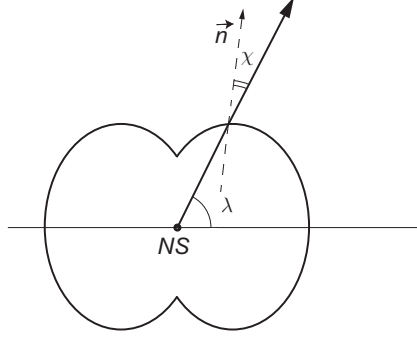


Figure 3: Schematics of the NS magnetosphere

3 Two regimes of plasma entering the NS magnetosphere

To enter the magnetosphere, the plasma in the shell must cool down from a high (almost virial) temperature T determined by hydrostatic equilibrium to some critical temperature T_{cr} [20]

$$\mathcal{R}T_{cr} = \frac{1}{2} \frac{\cos \chi}{\kappa R_A} \frac{\mu_m G M}{R_A} \quad (1)$$

Here \mathcal{R} is the universal gas constant, $\mu_m \approx 0.6$ is the molecular weight, G is the Newtonian gravitational constant, M is the neutron star mass, κ is the local curvature of the magnetosphere and χ is the angle between the outer normal and the radius-vector at any given point at the Alfvén surface (Fig. 3).

As was shown in [19, 21], a transition zone above the Alfvén surface with radius R_A is formed inside which the plasma cools down. The effective gravitational acceleration in this zone is

$$g_{eff} = \frac{GM}{R_A^2} \cos \chi \left(1 - \frac{T}{T_{cr}}\right) \quad (2)$$

and the mean radial velocity of plasma settling is

$$u_R = f(u) \sqrt{2GM/R_A}. \quad (3)$$

In the steady state, the dimensionless factor $0 \leq f(u) \leq 1$ is determined by the specific plasma cooling mechanism in this zone and, by conservation of mass, is constant through the shell. This factor can be expressed through the plasma cooling time t_{cool} in the transition zone [19]:

$$f(u) \simeq \left(\frac{t_{ff}}{t_{cool}}\right)^{1/3} \cos \chi^{1/3} \quad (4)$$

where $t_{ff} = R^{3/2} / \sqrt{2GM}$ is the characteristic free-fall time scale from radius R . The angle χ is determined by the shape of the magnetosphere, and for the magnetospheric boundary parametrized in the form $\sim \cos \lambda^n$ (where λ is the angle calculated from the magnetospheric equator, see Fig. 3) $\tan \chi = n \tan \lambda$. For example, in model calculations

by [16] $n \simeq 0.27$ in the near-equatorial zone, so $\kappa R_A \approx 1.27$. We see that $\cos \chi \simeq 1$ up to $\lambda \sim \pi/2$, so below (as in [19]) we shall omit $\cos \chi$.

Along with the density of matter near the magnetospheric boundary $\rho(R_A)$, the factor $f(u)$ determines the magnetosphere mass loading rate through the mass continuity equation:

$$\dot{M} = 4\pi R_A^2 \rho(R_A) f(u) \sqrt{2GM/R_A}. \quad (5)$$

This plasma eventually reaches the neutron star surface and produces an X-ray luminosity $L_x \approx 0.1 \dot{M} c^2$. Below we shall normalize the mass accretion rate through the magnetosphere as well as the X-ray luminosity to the fiducial values $\dot{M}_n \equiv \dot{M}/10^n \text{ g s}^{-1}$ and $L_n \equiv L_x/10^n \text{ erg s}^{-1}$, respectively.

3.1 The Compton cooling regime

As explained in detail in [19] (Appendix C and D), in subsonic quasi-static shells above slowly rotating NS magnetospheres the adiabaticity of the accreting matter is broken due to turbulent heating and Compton cooling. X-ray photons generated near the NS surface tend to cool down the matter in the shell via Compton scattering as long as the plasma temperature $T > T_x$, where T_x is the characteristic radiation temperature determined by the spectral energy distribution of the X-ray radiation. For typical X-ray pulsars $T_x \sim 3 - 5 \text{ keV}$. Cooling of the plasma at the base of the shell decreases the temperature gradient and hampers convective motions. Additional heating due to sheared convective motions is insignificant (see Appendix C of [19]). Therefore, the temperature in the shell changes with radius almost adiabatically $\mathcal{RT} \sim (2/5)GM/R$, and the distance R_x within which the plasma cools down by Compton scattering is

$$R_x \approx 10^{10} \text{ cm} \left(\frac{T_x}{3 \text{ keV}} \right)^{-1}, \quad (6)$$

, much larger than the characteristic Alfvén radius $R_A \approx 10^9 \text{ cm}$.

The Compton cooling time is inversely proportional to the photon energy density,

$$t_C \sim R^2/L_x, \quad (7)$$

and near the Alfvén surface we find

$$t_C \approx 10[\text{s}] \left(\frac{R_A}{10^9 \text{ cm}} \right)^2 L_{36}^{-1}. \quad (8)$$

(This estimate assumes spherical symmetry of the X-ray emission beam). Clearly, for the exact radiation density the shape of the X-ray emission produced in the accretion column near the NS surface (i.e. X-ray beam) is important, but still $L_x \sim \dot{M}$. Therefore, roughly, $f(u)_C \sim \dot{M}^{1/3}$, or, more precisely, taking into account the dependence of R_A on \dot{M} , in this regime

$$R_A^C \approx 10^9 \text{ cm} L_{36}^{-2/11} \mu_{30}^{6/11} \quad (9)$$

we obtain:

$$f(u)_C \approx 0.3 L_{36}^{4/11} \mu_{30}^{-1/11}. \quad (10)$$

Here $\mu_{30} = \mu/10^{30} \text{ G cm}^3$ is the NS dipole magnetic moment.

3.2 The radiative cooling regime

In the absence of a dense photon field, at the characteristic temperatures near the magnetosphere $T \sim 30$ -keV and higher, plasma cooling is essentially due to radiative losses (bremsstrahlung), and the plasma cooling time is $t_{rad} \sim \sqrt{T}/\rho$. Making use of the continuity equation (5) and the temperature distribution in the shell $T \sim 1/R$, we obtain

$$t_{rad} \sim R\dot{M}^{-1}f(u). \quad (11)$$

Note that, unlike the Compton cooling time (7), the radiative cooling time is actually independent of \dot{M} (remember that $\dot{M} \sim f(u)$ in the subsonic accretion regime!). Numerically, near the magnetosphere we have

$$t_{rad} \approx 1000[\text{s}] \left(\frac{R_A}{10^9 \text{cm}} \right) L_{36}^{-1} \left(\frac{f(u)}{0.3} \right). \quad (12)$$

Following the method described in Section 3 of [19], we find the mean radial velocity of matter entering the NS magnetosphere in the near-equatorial region, similar to the expression for $f(u)$ in the Compton cooling region Eq. (10). Using the expression for the Alfvén radius as expressed through $f(u)$, we calculate the dimensionless settling velocity:

$$f(u)_{rad} \approx 0.1 L_{36}^{2/9} \mu_{30}^{2/27} \quad (13)$$

and the Alfvén radius:

$$R_A^{rad} \simeq 10^9 [\text{cm}] L_{36}^{-2/9} \mu_{30}^{16/27} \quad (14)$$

(in the numerical estimates we assume a monoatomic gas with adiabatic index $\gamma = 5/3$). The obtained expression for the dimensionless settling velocity of matter Eq. (13) in the radiative cooling regime clearly shows that here accretion proceeds much less effectively than in the Compton cooling regime (cf. with Eq. (10)).

Unlike in the Compton cooling regime, in the radiative cooling regime there is no instability leading to an increase of the mass accretion rate as the luminosity increases (due to the long characteristic cooling time), and accretion here is therefore expected to proceed more quietly under the same external conditions.

4 Comparison with observations

4.1 High and low ('off') states in X-ray pulsars

So called 'off' states have been observed in several slowly rotating low luminosity pulsars such as Vela X-1 [22, 23, 24, 25], GX 301-2 [26] and 4U 1907+09 [27, 28, 29]. These states are characterized by a sudden, most often without any prior indication, drop in X-ray flux down to 1–10% of normal levels, lasting typically for a few minutes.

It seems to be fairly well established that the off states can not be simply due to increased absorption along the line of sight. Their occurrence is not correlated with increased N_H ([30],[28] but see also[31] for a another type of intensity dips in Vela X-1, most probably caused by dense blobs in the wind), the timescale of their onsets is too short (e.g.[24]) and spectral studies show a softening of the X-ray spectrum

during the off state [26, 25], contrary to what expected had the decreased flux levels been caused by increased absorption. Failure by early observations with instruments like *RXTE*/PCA to detect pulsations during the off states have seemed to suggest that the sources were instead simply turned off due to a sudden cessation of accretion. The popular view is that the cause of this may be large density variations in the stellar wind, possibly combined with the onset of the propeller regime (see e.g. [24]).

Recent observations with the more sensitive instruments onboard Suzaku of Vela X-1 [25] and 4U 1907+09 [29], however, show that although dropping in luminosity by a factor of about 20 the sources are clearly detected with pulse periods equal to those observed at normal flux levels. This suggests that rather than cessation of accretion, the off-states may be better explained by a transition to a different, less effective, accretion regime. We suggest that the onset of the off state in these sources marks a transition from the Compton cooling dominated to the radiative cooling dominated regime when the accretion rate drops below some value L_{\dagger} .

4.2 Switch between pencil and fan beam from the accretion column

A decrease in the X-ray photon energy density in the transition zone diminishes the Compton cooling efficiency, but the Compton cooling time remains much shorter than the radiative cooling time down to very low luminosities (see Eq. (8) and Eq. (12)). Therefore, in the spherically symmetric case, a transition between the two regimes would require an almost complete switch-off of Compton cooling in the equatorial magnetospheric region. In the more realistic non-spherical case, the Compton cooling time can become comparable to the radiation cooling time when the X-ray beam pattern changes with decreasing X-ray luminosity from a fan beam to a pencil beam, and the equatorial X-ray flux is reduced by a factor of a few. Additionally, hardening of the pulsed X-ray flux with decreasing X-ray luminosity, which is observed in low-luminosity X-ray pulsars [32], increases T_x and decreases the specific Compton cooling rate of the plasma $\propto (T - T_x)/t_C$, thus making Compton cooling less efficient. Such X-ray pattern transitions have been observed in transient X-ray pulsars (see, e.g., [33]). The radiation density in the X-ray pencil beam cools down the plasma predominantly in the magnetospheric cusp region, but because of the stronger magnetic line curvature [16] the plasma entry rate through the cusp will be insignificant. Still, the plasma continues to enter the magnetosphere via instabilities in the equatorial zone, but at a lower rate determined by the longer radiative cooling timescale. This is illustrated in Fig. 4.

The mass accretion rate in the radiative cooling regime will be determined by the plasma density by the time Compton cooling switches off in the magnetospheric equatorial region. This occurs at some X-ray luminosity $L_x \lesssim L_{\dagger}$, which can be estimated from the following considerations.

The transition from fan to pencil beam in low-luminosity X-ray pulsars with $L_x < 10^{37} \text{ erg s}^{-1}$, where no high accretion columns should exist, does not occur until the optical depth in the accretion flow above the polar cap becomes less than one. The optical depth in the accretion flow in the direction normal to the NS surface from the

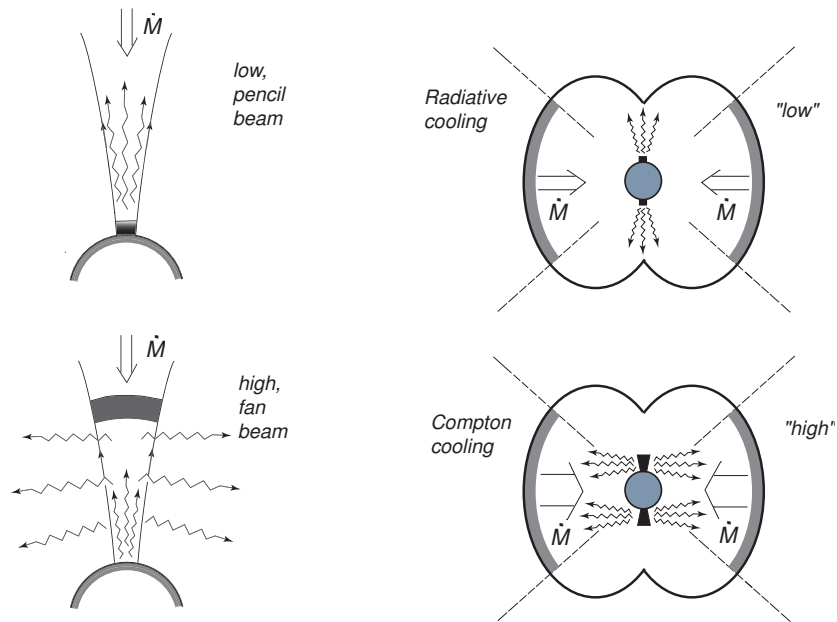


Figure 4: Schematics of the transition between the Compton ('high' state) and radiative ('low' state) plasma cooling regimes due to the X-ray beam switch from fan to pencil pattern with decreasing mass accretion rate.

radial distance $r_6 = r/10^6$ cm is estimated to be [34]

$$\tau_n \simeq 3 \left(\frac{R_A}{10^9 \text{ cm}} \right)^{1/2} \dot{M}_{16} r_6^{-3/2} \quad (15)$$

(here the NS mass is assumed to be $1.5 M_\odot$ and the NS radius $R_{NS} = 10^6$ cm). Taking into account the dependence of the Alfvén radius on \dot{M} and μ (see Eq. (9)), we see from this estimate that the X-ray emission beam change is expected to occur at $\tau_n < 1$, corresponding to an X-ray luminosity of

$$L_\dagger \sim 3 \times 10^{35} [\text{erg s}^{-1}] \mu_{30}^{-3/10}. \quad (16)$$

The return from radiative cooling dominated accretion back to the Compton cooling dominated regime can take place, for example, due to a density increase above the magnetosphere, leading to an increase in the mass accretion rate. The higher accretion rate leads to growth of the vertical optical depth of the accretion column, disappearance of the beam and enhancement of the lateral X-ray emission illuminating the magnetospheric equator (see Fig. 4). Therefore, the radiative energy density in the equatorial magnetospheric region strongly increases, Compton cooling resumes, and the source goes back to higher luminosity levels.

The idea that the transition between the two regimes may be triggered by a change in the X-ray beam pattern is supported by the pulse profile observations of Vela X-1 in different energy bands [25]. The observed change in phase of the 20–60 keV profile in the off-state (at X-ray luminosity $\sim 2.4 \times 10^{35} \text{ erg s}^{-1}$), reported by [25], suggests a disappearance of the fan beam at hard X-ray energies upon the source entering this state and the formation of a pencil beam (see [35] for more detailed discussion).

Note that the pulse profile phase change associated with X-ray beam switching below some critical luminosity, as observed in Vela X-1, seems to be suggested by an *XMM – Newton* observation of the SFXT IGR J11215–5952 (see Fig. 3 in [36]), corroborating the subsonic accretion regime with radiative plasma cooling at low X-ray luminosities in SFXTs as well, as we shall discuss in the next section.

4.3 SFXTs

Supergiant Fast X-ray Transients (SFXTs) are a subclass of HMXBs associated with early-type supergiant companions [37, 38, 39], and characterized by sporadic, short and bright X-ray flares reaching peak luminosities of 10^{36} – $10^{37} \text{ erg s}^{-1}$. Most of them were discovered by INTEGRAL [40, 41, 42, 43, 44, 45]. They show high dynamic ranges (between 100 and 10,000, depending on the specific source; e.g. [46, 47]) and their X-ray spectra in outburst are very similar to accreting pulsars in HMXBs. In fact, half of them have measured neutron star (NS) spin periods similar to those observed from persistent HMXBs (see [48] for a recent review).

The physical mechanism driving their transient behavior, related to the accretion by the compact object of matter from the supergiant wind, has been discussed by several authors and is still a matter of debate, as some of them require particular properties of the compact objects hosted in these systems [49, 50], and others assume peculiar clumpy properties of the supergiant winds and/or orbital characteristics [51, 52, 36, 53,

54, 55]. Recent studies of HMXB population in the Galaxy [56] suggested that SFXT activity should be connected to some accretion inhibition from the stellar wind.

Energy released in bright flares. The typical energy released in a SFXT bright flare is about $10^{38} - 10^{40}$ ergs [57], varying by one order of magnitude between different sources. That is, the mass fallen onto the NS in a typical bright flare varies from 10^{18} g to around 10^{20} g.

The typical X-ray luminosity outside outbursts in SFXTs is about $L_{x,low} \simeq 10^{34}$ erg s^{-1} [58], and below we shall normalise the luminosity to this value, L_{34} . At these low X-ray luminosities, the plasma entry rate into the magnetosphere is controlled by radiative plasma cooling. Further, it is convenient to normalise the typical stellar wind velocity from hot OB-supergiants v_w to 1000 km s^{-1} (for orbital periods of about a few days or larger the NS orbital velocities can be neglected compared to the stellar wind velocity from the OB-star), so that the Bondi gravitational capture radius is $R_B = 2GM/v_w^2 = 4 \times 10^{10} v_8^{-2}$ cm for a fiducial NS mass of $M_x = 1.5M_\odot$.

Let us assume that a quasi-static shell hangs over the magnetosphere around the NS, with the magnetospheric accretion rate being controlled by radiative plasma cooling. We denote the actual steady-state accretion rate as \dot{M}_a so that the observed X-ray steady-state luminosity is $L_x = 0.1\dot{M}_a c^2$. Then from the theory of subsonic quasi-spherical accretion [19] we know that the factor $f(u)$ (the ratio of the actual velocity of plasma entering the magnetosphere, due to the Rayleigh-Taylor instability, to the free-fall velocity at the magnetosphere, $u_{ff}(R_A) = \sqrt{2GM/R_A}$) reads [35, 21]

$$f(u)_{rad} \simeq 0.036 L_{34}^{2/9} \mu_{30}^{2/27}. \quad (17)$$

(See also Eq. (13) above).

The shell is quasi-static (and likely convective), unless something triggers a much faster matter fall through the magnetosphere (a possible reason is suggested below). It is straightforward to calculate the mass of the shell using the density distribution $\rho(R) \propto R^{-3/2}$ [19]. Using the mass continuity equation to eliminate the density above the magnetosphere, we readily find

$$\Delta M \approx \frac{2}{3} \frac{\dot{M}_a}{f(u)} t_{ff}(R_B). \quad (18)$$

Note that this mass can be expressed through measurable quantities $L_{x,low}$, μ_{30} and the (not directly observed) stellar wind velocity at the Bondi radius $v_w(R_B)$. Using Eq. (17) for the radiative plasma cooling, we obtain

$$\Delta M_{rad} \approx 8 \times 10^{17} [g] L_{34}^{7/9} v_8^{-3} \mu_{30}^{-2/27}. \quad (19)$$

The simple estimate (19) shows that for a typical wind velocity near the NS of about 500 km s^{-1} the *typical* mass of the hot magnetospheric shell is around 10^{19} g, corresponding to 10^{39} ergs released in a flare in which all the matter from the shell is accreted onto the NS, as observed. Clearly, variations in stellar wind velocity between different sources by a factor of ~ 2 would produce the one-order-of-magnitude spread in ΔM observed in bright SFXT flares.

In Fig. 5 we show the mean energy of SFXT bright flares $\Delta E = 0.1\Delta M c^2$ as a function of the low (non flaring) X-ray luminosity for nine SFXTs from our recent

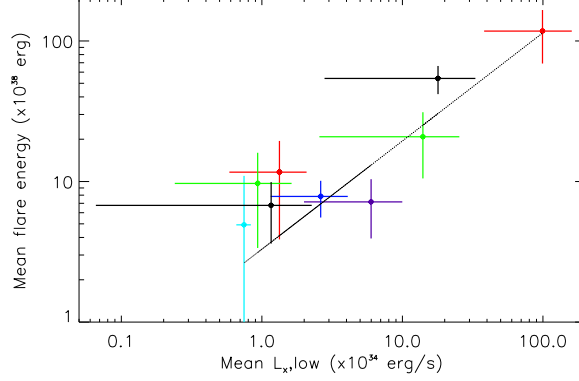


Figure 5: The mean energy released in bright flares (17 – 50 keV, data from [59]) versus average *INTEGRAL*/IBIS source luminosity. The *x-axis* is in units of 10^{34} erg s^{-1} , the *y-axis* is in units of 10^{38} ergs. The straight line gives the formal rms linear fit with the slope 0.77 ± 0.13 . (Figure adapted from [57]).

paper [57]. The low (non flaring) X-ray luminosity (*x-axis*) has been taken from [60], where a nine year time-averaged source flux in the 17–60 keV band is given for each source³. The data selection and analysis is discussed in detail in [59], together with the assumed distances and relevant references, so we refer the reader to that paper for the technical details. The uncertainties on the low luminosities include both the statistical errors on source fluxes, as reported in [60], and the known SFXTs distances and their uncertainties as reported by [59]. The formal rms fit to these points, shown by the straight line, gives the dependence of $\Delta E_{38} = (3.3 \pm 1.0)L_{34}^{0.77 \pm 0.13}$. This exactly corresponds to the radiative cooling regime $\Delta E \propto L^{7/9}$ (see Eq. (19)), as expected. A comparison with the coefficient in expression (19) suggests $v_8 \sim 0.62$, similar to typical wind velocities observed in HMXBs.

What can trigger SFXT flaring activity? As noted in [35], if there is an instability leading to a rapid fall of matter through the magnetosphere, a large quantity of X-ray photons produced near the NS surface should rapidly cool down the plasma near the magnetosphere, further increasing the plasma fall velocity $u_R(R_A)$ and the ensuing accretion NS luminosity L_x . Therefore, in a bright flare the entire shell can fall onto the NS on the free-fall time scale from the outer radius of the shell $t_{ff}(R_B) \sim 1000$ s. Clearly, the shell will be replenished by new wind capture, so the flares will repeat as long as the rapid mass entry rate into the magnetosphere is sustained.

Magnetized stellar wind as the flare trigger. We suggest that the shell instability described above can be triggered by a large-scale magnetic field sporadically carried by the stellar wind of the optical OB companion. Observations suggest that about $\sim 10\%$

³IGR J17544–2619, IGR J16418–4532, IGR J16479–4514, IGR J16465–4507, SAX J1818.6–1703, IGR J18483–0311, XTE J1739–302, IGR J08408–4503, IGR J18450–0435, IGR J18410–0535, IGR J11215–5952

of hot OB-stars have magnetic fields up to a few kG (see [61] for a recent review and discussion). It is also well known from Solar wind studies (see e.g. reviews [62, 63] and references therein) that the Solar wind patches carrying tangent magnetic fields has a lower velocity (about 350 km s^{-1}) than the wind with radial magnetic fields (up to $\sim 700 \text{ km s}^{-1}$). Fluctuations of the stellar wind density and velocity from massive stars are also known from spectroscopic observations [64], with typical velocity fluctuations up to $0.1 v_\infty \sim 200 - 300 \text{ km s}^{-1}$.

The effect of the magnetic field carried by the stellar wind is twofold: first, it may trigger rapid mass entry to the magnetosphere via magnetic reconnection in the magnetopause (the phenomenon well known in the dayside Earth magnetosphere, [65]), and secondly, the magnetized parts of the wind (magnetized clumps with a tangent magnetic field) have a lower velocity than the non magnetised ones (or the ones carrying the radial field). As discussed in [57] and below, magnetic reconnection can increase the plasma fall velocity in the shell from inefficient, radiative-cooling controlled settling accretion with $f(u)_{\text{rad}} \sim 0.03 - 0.1$, up to the maximum possible free-fall velocity with $f(u) = 1$. In other words, during a bright flare subsonic settling accretion turns into supersonic Bondi accretion. The second factor (slower wind velocity in magnetized clumps with tangent magnetic field) strongly increases the Bondi radius $R_B \propto v_w^{-2}$ and the corresponding Bondi mass accretion rate $\dot{M}_B \propto v_w^{-3}$.

Indeed, we can write down the mass accretion rate onto the NS in the unflaring (low-luminosity) state as $\dot{M}_{a,\text{low}} = f(u)\dot{M}_B$ with $f(u)$ given by expression (17) and $\dot{M}_B \simeq \pi R_B^2 \rho_w v_w$. Eliminating the wind density ρ_w using the mass continuity equation written for the spherically symmetric stellar wind from the optical star with power \dot{M}_o and assuming a circular binary orbit, we arrive at $\dot{M}_B \simeq \frac{1}{4} \dot{M}_o \left(\frac{R_B}{a}\right)^2$. Next, let us utilize the well-known relation for the radiative wind mass-loss rate from massive hot stars $\dot{M}_o \simeq \epsilon \frac{L}{c v_\infty}$ where L is the optical star luminosity, v_∞ is the stellar wind velocity at infinity, typically $2000\text{--}3000 \text{ km s}^{-1}$ for OB stars and $\epsilon \simeq 0.4 - 1$ is the efficiency factor [66] (in the numerical estimates below we shall assume $\epsilon = 0.5$). It is also possible to reduce the luminosity L of a massive star to its mass M using the phenomenological relation $(L/L_\odot) \approx 19(M/M_\odot)^{2.76}$ (see e.g. [67]). Combining the above equations and using Kepler's third law to express the orbital separation a through the binary period P_b , we find for the X-ray luminosity of SFXTs in the non-flaring state

$$L_{x,\text{low}} \simeq 5 \times 10^{35} [\text{erg s}^{-1}] f(u) \left(\frac{M}{10M_\odot}\right)^{2.76-2/3} \left(\frac{v_\infty}{1000 \text{ km s}^{-1}}\right)^{-1} \left(\frac{v_w}{500 \text{ km s}^{-1}}\right)^{-4} \left(\frac{P_b}{10 \text{ d}}\right)^{-4/3}, \quad (20)$$

which for $f(u) \sim 0.03 - 0.1$ corresponds to the typical low-state luminosities of SFXTs of $\sim 10^{34} \text{ erg s}^{-1}$.

It is straightforward to see that a transition from the low state (subsonic accretion with slow magnetospheric entry rate $f(u) \sim 0.03 - 0.1$) to supersonic free-fall Bondi accretion with $f(u) = 1$ due to the magnetized stellar wind with the velocity decreasing by a factor of two, for example, would lead to a flaring luminosity of $L_{x,\text{flare}} \sim (10 \div 30) \times 2^5 L_{x,\text{low}}$. This shows that the dynamical range of SFXT bright flares ($\sim 300 - 1000$) can be naturally reproduced by the proposed mechanism.

Conditions for magnetic reconnection. For magnetic field reconnection to oc-

cur, the time the magnetized plasma spends near the magnetopause should be at least comparable to the reconnection time, $t_r \sim R_A/v_r$, where v_r is the magnetic reconnection rate, which is difficult to assess from first principles [68]. For example, in the Petschek fast reconnection model $v_r = v_A(\pi/8 \ln S)$, where v_A is the Alfvén speed and S is the Lundquist number (the ratio of the global Ohmic dissipation time to the Alfvén time); for typical conditions near NS magnetospheres we find $S \sim 10^{28}$ and $v_r \sim 0.006v_A$. In real astrophysical plasmas the large-scale magnetic reconnection rate can be a few times as high, $v_r \sim 0.03 - 0.07v_A$ [68], and, guided by phenomenology, we can parametrize it as $v_r = \epsilon_r v_A$ with $\epsilon_r \sim 0.01 - 0.1$. The longest time-scale the plasma penetrating into the magnetosphere spends near the magnetopause is the instability time, $t_{inst} \sim t_{ff}(R_A)f(u)_{rad}$ [19], so the reconnection may occur if $t_r/t_{inst} \sim (u_{ff}/v_A)(f(u)_{rad}/\epsilon_r) \lesssim 1$. As near R_A (from its definition) $v_A \sim u_{ff}$, we arrive at $f(u)_{rad} \lesssim \epsilon_r$ as the necessary reconnection condition. According to Eq. (17), it is satisfied only at sufficiently low X-ray luminosities, pertinent to ‘quiet’ SFXT states. *This explains why in HMXBs with convective shells at higher luminosity (but still lower than $4 \times 10^{36} \text{ erg s}^{-1}$, at which settling accretion is possible), reconnection from magnetised plasma accretion will not lead to shell instability, but only to temporal establishment of the ‘strong coupling regime’ of angular momentum transfer through the shell, as discussed in [19].* Episodic strong spin-ups, as observed in GX 301-2, may be manifestations of such ‘failed’ reconnection-induced shell instability.

Therefore, it seems likely that the key difference between steady HMXBs like Vela X-1, GX 301-2 (showing only moderate flaring activity) and SFXTs is that in the first case the effects of possibly magnetized stellar winds from optical OB-companions are insignificant (basically due to the rather high mean accretion rate), while in SFXTs with lower ‘steady’ X-ray luminosity, large-scale magnetic fields, sporadically carried by clumps in the wind, can trigger SFXT flaring activity via magnetic reconnection near the magnetospheric boundary. The observed power-law SFXT flare distributions, discussed in [59], with respect to the log-normal distributions for classical HMXBs [69], may be related to the properties of magnetized stellar wind and physics of its interaction with the NS magnetosphere.

5 Conclusions

In [19, 70, 21] a theory of quasi-spherical wind accretion onto slowly rotating magnetized NS in binary systems was developed. It was shown that at luminosities below $\sim 4 \times 10^{36} \text{ erg s}^{-1}$, the accreting plasma does not cool before reaching the magnetosphere, so a hot quasi-static shell forms around the NS magnetosphere. This shell is likely to be convectively unstable and turbulent, which allows angular momentum to be transferred to/from the rotating magnetosphere causing NS spin-up/spin-down with specific behaviour as a function of the X-ray luminosity [19]. The theory is able to explain the observed spin-up/spin-down behavior and phenomenological correlations in slowly rotating moderately luminous X-ray pulsars (Vela X-1, GX 301-2 [19]), as well as the properties of the steady spin-down trend observed in GX 1+4 [71] and other slowly rotating low-luminosity X-ray pulsars (e.g. SXP 1062, 4U 2206 +54) [72] without invoking extremely strong NS magnetic fields.

In the settling accretion theory, the actual mass accretion rate through the shell is determined by the ability of the plasma to enter the NS magnetosphere via the Rayleigh-Taylor instability, which depends on the cooling mechanism. As shown in [35], the change between different plasma cooling regimes (from more efficient Compton cooling to less efficient radiative cooling) can occur when the X-ray luminosity decreases below some value $L_{\dagger} \sim 3 \times 10^{35} \text{ erg s}^{-1}$. This transition occurs mainly due to a switch of the X-ray beam pattern from a fan-like form generated by the accretion column (at high luminosities) to a pencil-like form (at low luminosities). This X-ray diagram switch is accompanied with an X-ray pulse profile shift, as observed during the temporal low-luminosity 'off' states in Vela X-1 [25], as well as in other slowly rotating accreting NSs (e.g. in the low states of SFXT IGR J11215–5952 [36]).

The subsonic settling accretion theory can also be applied to explain strongly non-stationary phenomena, including SFXT flares. As argued in [57], SFXT bright flares may be caused by sporadic transitions between different regimes of accretion in a quasi-spherical shell around a slowly rotating magnetized neutron star. The non-flaring steady states of SFXTs with low X-ray luminosity $L_{x,low} \sim 10^{32} - 10^{34} \text{ erg s}^{-1}$ may be associated with settling subsonic accretion mediated by ineffective radiative plasma cooling near the magnetospheric boundary. In this state, the accretion rate onto the neutron star is suppressed by a factor of ~ 30 relative to the Bondi-Hoyle-Littleton value. Changes in the local wind velocity and density due to, e.g., clumps, can only increase the mass accretion rate by a factor of $\sim 10 - 30$, bringing the system into the Compton cooling dominated regime, and lead to the production of moderately bright flares ($L_x \lesssim 10^{36} \text{ erg s}^{-1}$). To interpret the brightest flares ($L_x > 10^{36} \text{ erg s}^{-1}$) displayed by the SFXTs within the quasi-spherical settling accretion regime, a larger increase in the mass accretion rate can be produced by sporadic capture of magnetized stellar wind plasma. Such episodes should not be associated with specific binary orbital phases, as observed in e.g. IGR J17544-2619 [73]. At sufficiently low accretion rates, magnetic reconnection can enhance the magnetospheric plasma entry rate, resulting in copious production of X-ray photons, strong Compton cooling and ultimately in unstable accretion of the entire shell. A bright flare develops on the free-fall time scale in the shell, and the typical energy released in an SFXT bright flare corresponds to the entire mass of the shell. This view is consistent with the energy released in SFXT bright flares ($\sim 10^{38} - 10^{40} \text{ ergs}$), their typical dynamic range ($\sim 100 - 1000$), and with the observed dependence of these characteristics on the average unflaring X-ray luminosity of SFXTs. Thus the flaring behaviour of SFXTs, as opposed to steady HMXBs, can be primarily related to their low X-ray luminosity in the settling accretion regime, allowing sporadic magnetic reconnection to occur during magnetized plasma entry to the NS magnetosphere.

We conclude that the settling regime of accretion onto NSs in wind-accreting close binary systems with moderate and low X-ray luminosity is now supported by different types of observations. There are likely to be more to come with the ever increasing quality of X-ray observations of accreting magnetised neutron stars.

Acknowledgement. The work is supported by the Russian Science Foundation grant 14-12-00146.

References

- [1] R. Giacconi, H. Gursky, F. R. Paolini, and B. B. Rossi, *Physical Review Letters* **9**, 439 (1962).
- [2] R. Giacconi, *Reviews of Modern Physics* **75**, 995 (2003).
- [3] Y. B. Zel’dovich and N. I. Shakura, *Sov. Astron.* **13**, 175 (1969).
- [4] R. Giacconi, H. Gursky, E. Kellogg, E. Schreier, and H. Tananbaum, *ApJL* **167**, L67 (1971).
- [5] H. Bradt and R. Giacconi, (Eds.), *X- and gamma-ray astronomy, proceedings of IAU Symposium no. 55 held in Madrid, Spain, 11-13 May 1972., IAU Symposium*, vol. 55 (1973) (1973).
- [6] A. Hewish, S. J. Bell, J. D. H. Pilkington, P. F. Scott, and R. A. Collins, *Nature* **217**, 709 (1968).
- [7] T. Gold, *Nature* **218**, 731 (1968).
- [8] P. Goldreich and W. H. Julian, *ApJ* **157**, 869 (1969).
- [9] N. I. Shakura, *Sov. Astron.* **16**, 756 (1973).
- [10] J. E. Pringle and M. J. Rees, *A&A* **21**, 1 (1972).
- [11] N. I. Shakura and R. A. Sunyaev, *A&A* **24**, 337 (1973).
- [12] D. Lynden-Bell, *Nature* **223**, 690 (1969).
- [13] B. A. Fryxell and R. E. Taam, *ApJ* **335**, 862 (1988).
- [14] M. Ruffert, *A&A* **346**, 861 (1999).
- [15] T. Nagae, K. Oka, T. Matsuda, H. Fujiwara, I. Hachisu, and H. M. J. Boffin, *A&A* **419**, 335 (2004).
- [16] J. Arons and S. M. Lea, *ApJ* **207**, 914 (1976).
- [17] A. F. Illarionov and R. A. Sunyaev, *A&A* **39**, 185 (1975).
- [18] D. J. Burnard, J. Arons, and S. M. Lea, *ApJ* **266**, 175 (1983).
- [19] N. Shakura, K. Postnov, A. Kochetkova, and L. Hjalmarsson, *MNRAS* **420**, 216 (2012).
- [20] R. F. Elsner and F. K. Lamb, *ApJ* **215**, 897 (1977).
- [21] N. I. Shakura, K. A. Postnov, A. Y. Kochetkova, and L. Hjalmarsson, in *European Physical Journal Web of Conferences, European Physical Journal Web of Conferences*, vol. 64 (2014), *European Physical Journal Web of Conferences*, vol. 64, 2001.

- [22] H. Inoue, Y. Ogawara, I. Waki, T. Ohashi, S. Hayakawa, H. Kunieda, F. Nagase, and H. Tsunemi, *PASJ* **36**, 709 (1984).
- [23] I. Kreykenbohm, P. Kretschmar, J. Wilms, R. Staubert, E. Kendziorra, D. E. Gruber, W. A. Heindl, and R. E. Rothschild, *A&A* **341**, 141 (1999).
- [24] I. Kreykenbohm, J. Wilms, P. Kretschmar, J. M. Torrejón, K. Pottschmidt, M. Hanke, A. Santangelo, C. Ferrigno, and R. Staubert, *A&A* **492**, 511 (2008).
- [25] V. Doroshenko, A. Santangelo, and V. Suleimanov, *A&A* **529**, A52 (2011).
- [26] E. Göğüş, I. Kreykenbohm, and T. M. Belloni, *A&A* **525**, L6 (2011).
- [27] J. J. M. in 't Zand, T. E. Strohmayer, and A. Baykal, *ApJL* **479**, L47 (1997).
- [28] Ş. Şahiner, S. Ç. Inam, and A. Baykal, *MNRAS* **421**, 2079 (2012).
- [29] V. Doroshenko, A. Santangelo, L. Ducci, and D. Klochkov, *A&A* **548**, A19 (2012).
- [30] F. Fürst, I. Kreykenbohm, S. Suchy, L. Barragán, J. Wilms, R. E. Rothschild, and K. Pottschmidt, *A&A* **525**, A73 (2011).
- [31] P. Kretschmar, I. Kreykenbohm, J. Wilms, R. Staubert, W. A. Heindl, D. E. Gruber, and R. E. Rothschild, in *American Institute of Physics Conference Series, American Institute of Physics Conference Series*, vol. 510 (Edited by M. L. McConnell and J. M. Ryan) (2000), *American Institute of Physics Conference Series*, vol. 510, 163–167.
- [32] D. Klochkov, R. Staubert, A. Santangelo, R. E. Rothschild, and C. Ferrigno, *A&A* **532**, A126 (2011).
- [33] A. N. Parmar, N. E. White, and L. Stella, *ApJ* **338**, 373 (1989).
- [34] F. K. Lamb, C. J. Pethick, and D. Pines, *ApJ* **184**, 271 (1973).
- [35] N. Shakura, K. Postnov, and L. Hjalmarsdotter, *MNRAS* **428**, 670 (2013).
- [36] L. Sidoli, P. Romano, S. Mereghetti, A. Paizis, S. Vercellone, V. Mangano, and D. Götz, *A&A* **476**, 1307 (2007).
- [37] L. J. Pellizza, S. Chaty, and I. Negueruela, *A&A* **455**, 653 (2006).
- [38] S. Chaty, F. Rahoui, C. Foellmi, J. A. Tomsick, J. Rodriguez, and R. Walter, *A&A* **484**, 783 (2008).
- [39] F. Rahoui, S. Chaty, P.-O. Lagage, and E. Pantin, *A&A* **484**, 801 (2008).
- [40] M. Chernyakova, A. Lutovinov, F. Capitanio, N. Lund, and N. Gehrels, *The Astronomer's Telegram* **157**, 1 (2003).
- [41] S. Molkov, N. Mowlavi, A. Goldwurm, A. Strong, N. Lund, J. Paul, and T. Oosterbroek, *The Astronomer's Telegram* **176**, 1 (2003).

- [42] R. A. Sunyaev, S. A. Grebenev, A. A. Lutovinov, J. Rodriguez, S. Mereghetti, D. Gotz, and T. Courvoisier, *The Astronomer's Telegram* **190**, 1 (2003).
- [43] S. A. Grebenev, A. A. Lutovinov, and R. A. Sunyaev, *The Astronomer's Telegram* **192**, 1 (2003).
- [44] V. Sguera, E. J. Barlow, A. J. Bird, D. J. Clark, A. J. Dean, A. B. Hill, L. Moran, S. E. Shaw, D. R. Willis, A. Bazzano, P. Ubertini, and A. Malizia, *A&A* **444**, 221 (2005).
- [45] I. Negueruela, D. M. Smith, P. Reig, S. Chaty, and J. M. Torrejón, in *Proc. of the "The X-ray Universe 2005"*, Ed. by A. Wilson. *ESA SP-604, Vol. 1, 2006* (2006), 165.
- [46] P. Romano, V. La Parola, S. Vercellone, G. Cusumano, L. Sidoli, H. A. Krimm, C. Pagani, P. Esposito, E. A. Hoversten, J. A. Kennea, K. L. Page, D. N. Burrows, and N. Gehrels, *MNRAS* **410**, 1825 (2011).
- [47] P. Romano, H. A. Krimm, D. M. Palmer, L. Ducci, P. Esposito, S. Vercellone, P. A. Evans, C. Guidorzi, V. Mangano, J. A. Kennea, S. D. Barthelmy, D. N. Burrows, and N. Gehrels, *A&A* **562**, A2 (2014).
- [48] L. Sidoli, in *Proc. 9th INTEGRAL Workshop. Published online at "http://pos.sissa.it/cgi-bin/reader/conf.cgi?confid=176"*, id.11 (2012).
- [49] S. A. Grebenev and R. A. Sunyaev, *Astronomy Letters* **33**, 149 (2007).
- [50] E. Bozzo, M. Falanga, and L. Stella, *ApJ* **683**, 1031 (2008).
- [51] J. J. M. in't Zand, *A&A* **441**, L1 (2005).
- [52] R. Walter and J. Zurita Heras, *A&A* **476**, 335 (2007).
- [53] I. Negueruela, J. M. Torrejón, P. Reig, M. Ribó, and D. M. Smith, in *AIP Conf. Ser.*, vol. 1010 (Edited by R. M. Bandyopadhyay, S. Wachter, D. Gelino, and C. R. Gelino) (2008), vol. 1010, 252–256.
- [54] L. Ducci, L. Sidoli, S. Mereghetti, A. Paizis, and P. Romano, *MNRAS* **398**, 2152 (2009).
- [55] L. M. Oskinova, A. Feldmeier, and P. Kretschmar, *MNRAS* **421**, 2820 (2012).
- [56] A. A. Lutovinov, M. G. Revnivtsev, S. S. Tsygankov, and R. A. Krivonos, *MNRAS* **431**, 327 (2013).
- [57] N. Shakura, K. Postnov, L. Sidoli, and A. Paizis, *MNRAS* **442**, 2325 (2014).
- [58] L. Sidoli, P. Romano, V. Mangano, A. Pellizzoni, J. A. Kennea, G. Cusumano, S. Vercellone, A. Paizis, D. N. Burrows, and N. Gehrels, *ApJ* **687**, 1230 (2008).
- [59] A. Paizis and L. Sidoli, *MNRAS* **439**, 3439 (2014).

- [60] R. Krivonos, S. Tsygankov, A. Lutovinov, M. Revnivitsev, E. Churazov, and R. Sunyaev, *A&A* **545**, A27 (2012).
- [61] J. Braithwaite, ArXiv e-prints (2013).
- [62] L. M. Zelenyi and A. V. Milovanov, *Physics Uspekhi* **47**, 1 (2004).
- [63] R. Bruno and V. Carbone, *Living Reviews in Solar Physics* **10** (2013).
- [64] J. Puls, J. S. Vink, and F. Najarro, *Astron. Astrophys. Rev.* **16**, 209 (2008).
- [65] J. W. Dungey, *Physical Review Letters* **6**, 47 (1961).
- [66] H. J. G. L. M. Lamers, E. P. J. van den Heuvel, and J. A. Petterson, *A&A* **49**, 327 (1976).
- [67] E. A. Vitrichenko, D. K. Nadyozhin, and T. L. Razinkova, *Astronomy Letters* **33**, 251 (2007).
- [68] E. G. Zweibel and M. Yamada, *ARAA* **47**, 291 (2009).
- [69] F. Fürst, I. Kreykenbohm, K. Pottschmidt, J. Wilms, M. Hanke, R. E. Rothschild, P. Kretschmar, N. S. Schulz, D. P. Huenemoerder, D. Klochkov, and R. Staubert, *A&A* **519**, A37 (2010).
- [70] N. I. Shakura, K. A. Postnov, A. Y. Kochetkova, and L. Hjalmarsson, *Physics-Uspekhi* **56**, 321 (2013).
- [71] A. González-Galán, E. Kuulkers, P. Kretschmar, S. Larsson, K. Postnov, A. Kochetkova, and M. H. Finger, *A&A* **537**, A66 (2012).
- [72] K. A. Postnov, N. I. Shakura, A. Y. Kochetkova, and L. Hjalmarsson, in *European Physical Journal Web of Conferences*, *European Physical Journal Web of Conferences*, vol. 64 (2014), *European Physical Journal Web of Conferences*, vol. 64, 2002.
- [73] S. P. Drave, A. J. Bird, L. Sidoli, V. Sguera, A. Bazzano, A. B. Hill, and M. E. Goossens, *MNRAS* **439**, 2175 (2014).

